Наносистеми, наноматеріали, нанотехнології
Nanosistemi, Nanomateriali, Nanotehnologii
2025, т. 23, № 4, сс. 1095–1105
https://doi.org/10.15407/nnn.23.04.1095

PACS numbers: 07.60.Rd, 61.05.cp, 68.37.Hk, 78.20.Ci, 78.40.Fy, 78.67.Sc, 85.60.Gz

Response of Self-Powered CuS/Si-Nanostructured-Heterojunction Photodetectors to Green Light at 530 nm

Sabah Salman Hamdi[1], Huda Saadi Ali[2], and Iftikhar Mahmood Ali[3]

[1]*College of Computer Science and Mathematics,*
University of Tikrit,
Salahddin Str.,
3400 Tikrit, Iraq
[2]*College of Energy and Environmental Sciences,*
Department of Renewable Energy,
Al-Karkh University of Science,
Haifa Str.,
Al-Karkh, Iraq
[3]*College of Science, Physics Department,*
University of Baghdad,
Al-Jadriya Str.,
Baghdad, Iraq

This study uses a series of CuS/Si-heterojunction self-powered visible-light photodetectors through chemical spray pyrolysis (CSP) technique at a substrate temperature of 300°C. The thickness of the prepared thin films is of about 228.4 nm measured by cross-sectional thickness. Various characterization techniques are used to investigate the structural and optical properties of the prepared thin films. The XRD results show that the CuS film has a polycrystalline nature, covellite-hexagonal structure, and preferred orientation along (100) planes. FESEM results show the formation of nanostructures consisting of stone-like shapes. The UV-visible absorbance spectra are recorded in range 300–1100 nm to investigate the optical characteristics. The results show that the absorption-coefficient value is $\alpha > 10^4$ for film that, in turn, proves that the prepared thin films are likely to have direct electronic transitions. The value of the optical energy gap is of 2.58 eV. Simultaneously, diode behaviour is illustrated by voltage-current characteristic. Also, the manufactured layers show an excellent figure of merit as a function of wavelength. The optical response is $R = 16.881$ μA/W and the specific detectivity is $D^* = 9.25 \cdot 10^{16}$ Jones, and the highest quantum-efficiency value is of 39.495 at 530 nm. The well-directed response at the wavelength of 530 nm indicates that the *p*-CuS/*n*-Si heterogeneous photodetectors have a great potential for applications. This sensitivity to green light indicates that these photodetectors

are particularly effective at detecting green wavelengths.

У цьому дослідженні використовується серія фотодетекторів видимого світла з власним живленням на основі гетеропереходу CuS/Si, одержаних методом хемічної розпорошувальної піролізи (CSP) за температури підкладинки у 300°C. Товщина одержаних тонких плівок становила близько 228,4 нм, виміряна за товщиною поперечного перерізу. Для дослідження структурних та оптичних властивостей одержаних тонких плівок було використано різні методи характеризації. Результати рентґенівської дифракції (XRD) показали, що плівка CuS має полікристалічну природу, ковеллінового типу гексагональну структуру та переважну орієнтацію вздовж площин типу (100). Результати сканівної електронної мікроскопії (FESEM) показали утворення наноструктур, що складаються з каменеподібних форм. Спектри вбирання в УФ-видимому діяпазоні було записано в діяпазоні 300–1100 нм для дослідження оптичних характеристик. Результати показали, що значення коефіцієнта вбирання становить $\alpha > 104$ для плівки, що, у свою чергу, довело, що одержані тонкі плівки, ймовірно, мають прямі електронні переходи. Значення оптичної забороненої щілини становило 2,58 еВ. Одночасно поведінка діоди ілюструється залежністю напруги від струму. Також виготовлені шари продемонстрували чудову залежність якости від довжини хвилі. Оптична чутливість становила $R = 16{,}881$ мкА/Вт, питома виявлювальна здатність — $D^* = 9{,}25 \cdot 10^{16}$ Джонс, а найвище значення квантової ефективности становило 39,495 на довжині хвилі у 530 нм. Добре спрямована чутливість на довжині хвилі у 530 нм вказує на те, що гетерогенні фотодетектори p-CuS/n-Si мають великий потенціял для застосування. Ця чутливість до зеленого світла вказує на те, що ці фотодетектори особливо ефективні для виявлення зелених довжин хвиль.

Key words: copper sulphide, voltage–current characteristic, spectral response, rise time, optical characteristics.

Ключові слова: сульфід Купруму, вольтамперна характеристика, спектральна чутливість, час наростання, оптичні характеристики.

(Received 26 July, 2024; in revised form, 11 September, 2024)

1. INTRODUCTION

CuS is an important direct-band gap p-type semiconductor that is often widely used in solar cells [1], batteries, supercapacitors, and photocatalysis [2] due to its excellent optical and electrical properties. Furthermore, the Cu and S elements, which make up CuS, are abundant on the earth and non-toxic. This is why CuS has gradually gained attention in recent years. There is strong mixing between the s- and p-orbitals of S and external s- and p-orbitals of Cu that results in the bonding bonds showing covalent-bonding properties

rather than ionic properties [3, 4]. According to reports, most of the chalcogenides, the compound Cu_xS has many phases depending on the compounds' ratio of copper to sulphur. There is the compound Cu_xS at room temperature with five known stable phases starting from the phase of chalcocite Cu_2S. The copper-rich phase has an orthorhombic system, the digenite phase has a cubic system, and the anillite phase has a cubic system and ends with the sulphur-rich covellite phase CuS and has a hexagonal system [3, 4]. Capriati CuS is characterized by the fact that it crystallizes in a hexagonal form and is found in the form of mass, thin layers, or granules spread in other copper metals, with a density of 4.6–4.76 g/cm^3. The CuS thin film is of great importance in industrial applications, where photovoltaic applications are used to manufacture solar cells, which are important new energy sources. The most famous solar cells are the CdS/Cu_xS; the preferred phase in these cells is chalcocite Cu_2S as well as cell $Cu_xS/(Cd,Zn)S$ [4–6], and it is also used in thermal photovoltaic (photothermic) conversion for solar energy, and thin film of CuS also works as absorbing coatings for sunlight, where they have a high absorption coefficient of visible wavelengths and are used as selective radiation filters on architectural windows for the control of solar radiation in warm climates, and good reflectivity of infrared wavelengths that has been used in thermal-mirror coatings; in addition, these thin films can be used as electrically-conductive coatings coated with organic polymers [7, 8] and in the manufacture of compounds involved in multidevice and multilayer structures (multijunction-type multilayer heterojunctions) [9].

2. EXPERIMENTAL DETAILS

In this work, copper sulphide nanoparticles were prepared at 200°C using the chemical pyrolysis spray method. Firstly, 0.005 M $CuCl_2{\cdot}2H_2O$ was dissolved in 100 ml of deionized water, and 0.01 ml of thiourea $Cs(NH_2)_2$ was dissolved in 100 ml of deionized water as starting materials for Cu and S ion sources. After that, an equal volumetric ratio (1:1) of both solutions is taken and mixed; the solutions are placed on magnetic stirrer for 10 min to ensure complete dissolution and obtain a homogeneous and transparent blue solution. Finally, copper-sulphide nanoparticles were obtained.

CuS solution is deposited on Si substrates at a temperature of 200°C. The distance between the nozzle and substrates is of 28 cm because more than that causes the evaporation of material before it reaches the bases. The *n*-Si wafer has electrical resistivity of 1–10 Ω·cm with (111) orientation and thickness of 500 ± 25 μm, when it was cut into pieces of 1.25×1.25 cm^2 dimensions and was cleaned with HF acid diluted with methanol in a ratio of 1:9, left Si sub-

strates inside this acidic solution for a minute and then rinse with distilled water and repeated cleaning with distilled water for 3 times to ensure the disposal of the remnants of the solution, after which the samples were dried well, CuS films were deposited at a substrate, and samples were annealed at 300°C for half an hour.

The *p*-CuS/*n*-Si heterojunction was prepared by chemical pyrolysis spray method. Aluminium electrodes were deposited by vacuum thermal-evaporation system under low pressure of about $5 \cdot 10^{-5}$ mPa and thickness of 200 nm. Aluminium electrodes were deposited on top of the films, and the silicon underside and the shape of the prepared photodetector became as in the illustrating diagrams below.

Optical measurements for all prepared films have been done using a spectrometer type UV-visible spectra photometer-1800 for the wavelength range 180–1100 nm. The current–voltage (*I*–*V*) characteristics are investigated using a 2450 Keithley electrometer.

3. RESULTS AND DISCUSSION

3.1. Structure

The results of x-ray diffraction (XRD) for the CuS film and the hexagonal system are shown in the preferred growth direction (100) (Fig. 1) of the film. Peak positions at the angles $2\theta \cong 25.32$, 32.82, 33.94, 39.39, 49.64, 68.26 correspond to (100), (102), (103), (105), (108), and (1011), respectively, and this is consistent with the results of the study [11], which have been compared with the standard card (ICDD) numbered (00-006-0464) for copper sulphide.

Table shows the structural parameters for standard peaks. The average crystallite size is calculated using the Scherer equation [12]

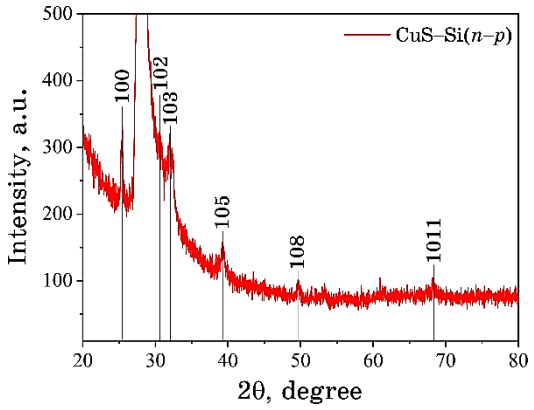

Fig. 1. Thin CuS/Si film XRD-pattern preparation.

TABLE. Structural parameters of *p*-CuS/*n*-Si.

Sample	2Θ	*hkl*	D_{hkl}, Å	*FWHM*	*D*, nm
CuS	25.32	(100)	3.558	0.3464	27.0
	32.78	(102)	2.728	0.3464	24.98
	33.94	(103)	2.641	0.1732	50.11
	39.39	(105)	2.28	0.4224	18.6
	49.64	(108)	1.83	0.6336	12.3
	68.26	(1011)	1.37	0.6336	13.6

$$D_{\text{ave}} = 0.9\lambda/(\beta\cos\theta), \quad (1)$$

where $\lambda = 1.5406$ Å is the x-ray wavelength (K_α-line), θ is the Bragg's diffraction angle, β [in radians] is the full-width at half-maximum (also called *FWHM*); it was found that the measured crystallite size values fall within the range 6.8–50.11 nm.

Through the study of the surface morphology of the prepared film by SEM, it is clear from Fig. 2, *a*, *b*, *c* that the film structure consists of stone-like shapes of nanostructured very regularly and that the surfaces of the prepared films have homogeneous distribution, dense, and free of spaces or characteristic islands; this is consistent with [11, 16].

The film thickness was measured using the cross-section technique in the scanning electron microscope device. It was found that the film features are uniform and moderately deposited. The average thickness of the film is of 228.4 nm, as shown in Fig. 2, *b*.

3.2. Optical Properties

Figures 3, *a*, *b* show the absorption and absorbance coefficients, respectively. As seen, the absorption spectra as a function of wavelength. The findings indicated that the films exhibited the most excellent absorbance level in the visible range of the electromagnetic spectrum, specifically between 300 and 700 nm. This is consistent with the information shown in Fig. 6, *a*, which relates to the sensitivity of a material to light.

The results showed that the absorption coefficient increases with the increase in photon energy of the prepared films, as the greatest values of the absorption coefficient are at high photon energies of 4–4.3 eV; this indicates the occurrence of the absorption process in this range (which includes the optical absorption edge) and the possibility of electronic transitions between the valence and conduction bands.

All these results are consistent with the data of studies [13, 14].

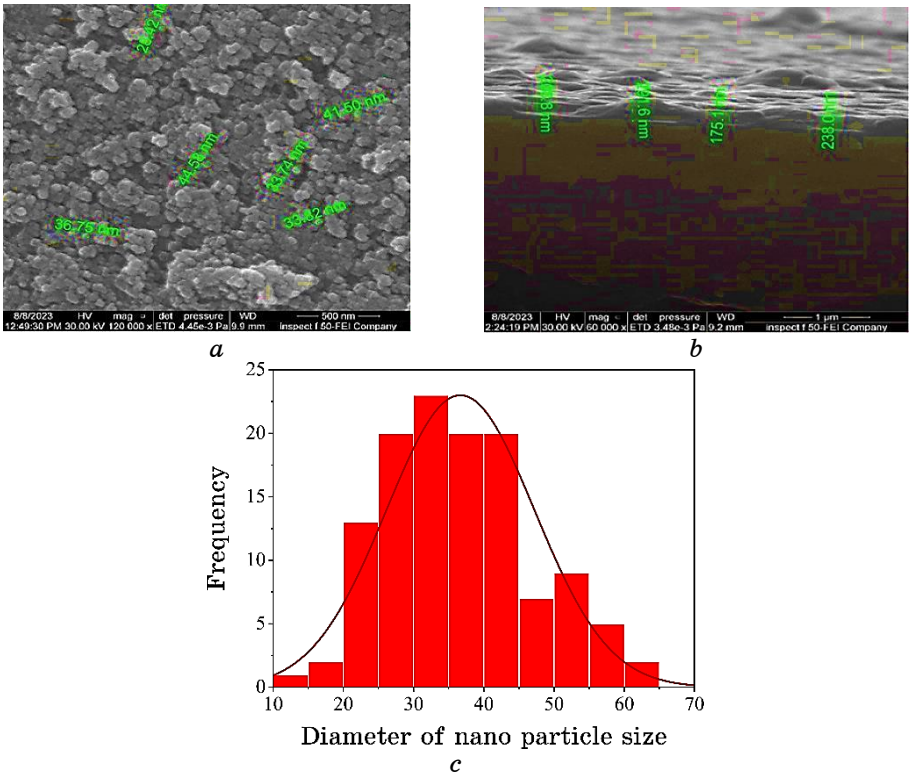

Fig. 2. CuS/Si thin film (*a*) FESEM pattern preparation, (*b*) cross section of CuS deposited on *n*-Si, (*c*) granular distribution rate.

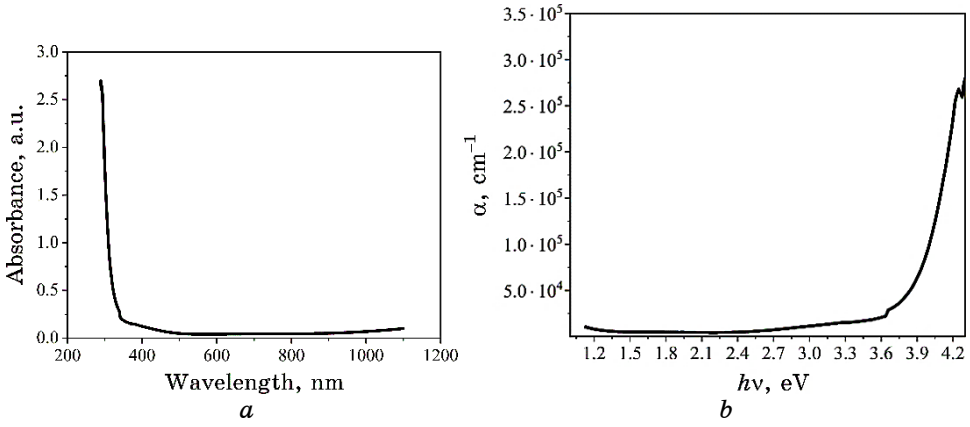

Fig. 3. (*a*) The absorption of CuS; (*b*) the absorption coefficient of CuS.

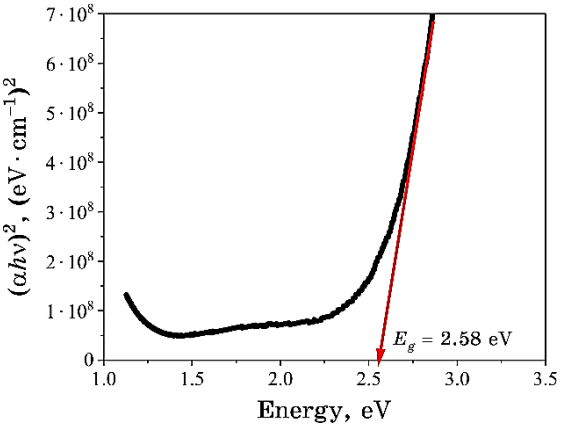

Fig. 4. A Tauc plot for the energy gap of CuS.

The energy gap value was calculated to estimate the difference between the valence and conduction bands, which can help determine the materials' electrical, thermal, and electronic properties.

The Tauc formula in Eq. (2) determines the direct energy gap:

$$\alpha h\nu = \beta\left(h\nu - E_g\right)^r, \tag{2}$$

where β is a constant, α is the absorption coefficient; $h\nu$ is the incident photon's energy; E_g is the optical bandgap, and $r = 1/2$ is the direct allowed transition.

Since the transitions are of the direct allowed type, *i.e.*, the value of the constant $r = 1/2$, and by drawing the relationship between $(\alpha h\nu)^2$ and the energy of the incident photon $h\nu$, through the extension of the straight part of the curve to determine the point of intersection of $(\alpha h\nu)^2$ with the *Ox* axis of the photon energy $h\nu$, where $(\alpha h\nu)^2 = 0$, that represents the value of the optical energy gap and, as shown in Fig. 4, where it was found, the optical energy-gap value of copper sulphide with a thickness of 228.4 nm for these films was of 2.58 eV corresponding to Eq. (2), which represents the Tauc equation, and this is consistent with Refs. [8, 18].

3.3. Spectral Response Characteristics

Figure 5 shows the voltage–current behaviour achieved in the *p*–*n* visible-light detector, where the emission current was reached in the dark and illumination at wavelengths of 405–460–500–530–575–625–720 nm. A decrease in emission current was observed; af-

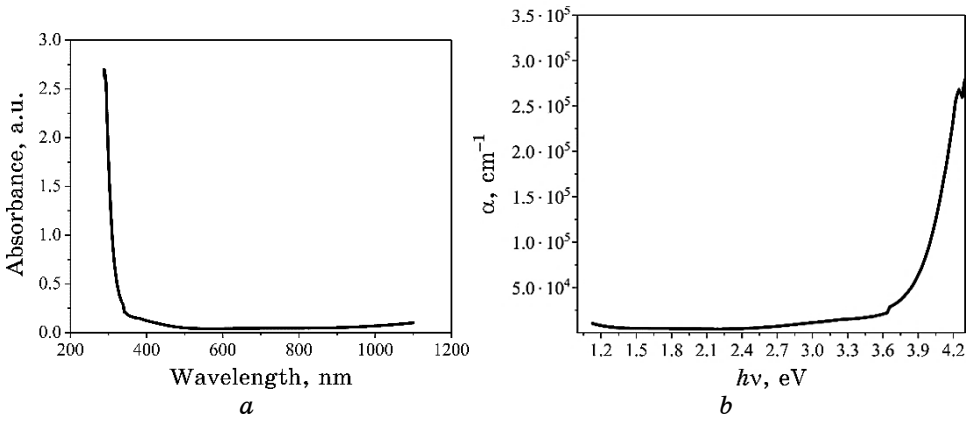

Fig. 5. Current–voltage characteristics of the fabricated CuS/Si photodetector.

ter that, an improved value was reached under lighting, and this can be detected by the spectral response, R, which represents the ratio of acquired light current/applied light intensity, $I_{ph}/P_{illumination}$. R is one of the important detector parameters, especially, with the large energy gap, by which the spectral range through which the detector operates, and Fig. 6, *a* shows the spectral response for heterojunction CuS/Si. We find that the highest value of R is $R = 16.881$ μA/W at the wavelength of 530 nm to the absorption of light of these lengths in the depletion zone and on its edges, but after the wavelength of 530 nm, the response decreases with increasing wavelength, where the film is transparent, and as a result, the response decreases. The increase in spectral response can be attributed to the enlargement of atomic size, enhanced growth rate, reduction in crystal defects, increased film thickness, and improved crystal structure.

Figure 6, *b* depicts the specific detectivity D^*, which is calculated using the expression $R/(2eI_D)^{1/2}$, where e is the charge of a free electron ($1.6 \cdot 10^{19}$ C) and I_D is the dark current [15, 19]. The CuS film exhibited an energy gap of 2.58 eV corresponding to a wavelength of 496 nm. This is calculated in Fig. 4 and is closest to the wavelength of the light source used in the experiment. The highest D^* value, $9.25 \cdot 10^{16}$ Jones, was observed at a wavelength of 530 nm. An increase in detectivity indicates fewer structural defects and reduced noise current significantly improving detectivity. Figure 6, *c* illustrates the quantum efficiency of the detector, which remaps the behaviour of R and D^*, accordingly. The maximum quantum efficiency calculated as $(I_{ph}/e)(P_{illumination}h\nu) \cdot 100\%$ was of 39.495 at 530 nm. This increase in quantum efficiency at the incident wave-

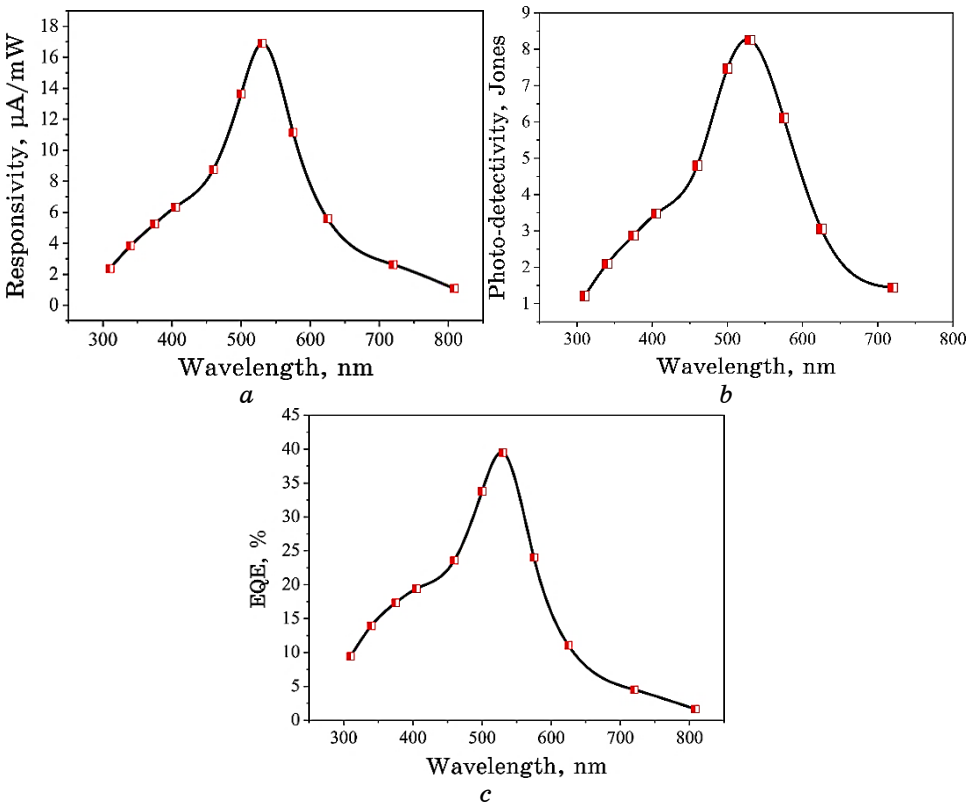

Fig. 6. (*a*) Photoresponsivity, (*b*) photodetectivity, and (*c*) external quantum efficiency of the fabricated CuS/Si photodetector.

length is due to reduced structural defects. Both R and D^* are critical for evaluating a photodetector light response and sensitivity performances, while the external quantum efficiency (EQE) assesses the detector efficiency in converting photons into electric current.

Under dark and illuminated conditions, across three iterations with a pulse width (of 25 sec), the time-dependent property of *p*-CuS/*n*-Si visible-light detector was measured. The detector exhibited a strong response over three cycles, demonstrating a significant response time. The response time/full time ratio was found to be of 0.32 and 0.65 seconds, indicating a relatively fast electron injection and slower electrons/holes [16, 17, 19], as shown in Fig. 7, *a*, *b*.

4. CONCLUSION

The CuS/Si heterojunction self-powered visible-light photodetector

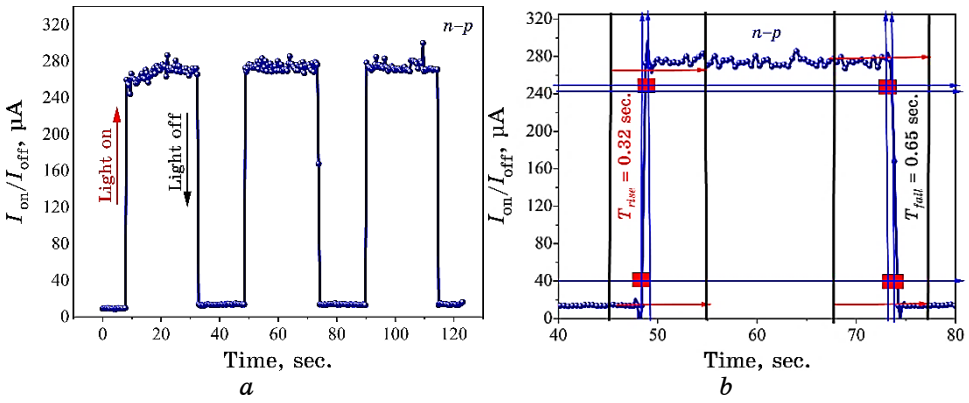

Fig. 7. (*a*) Switching behaviour and (*b*) response/recovery time of the fabricated CuS/Si photodetector.

exhibited high efficiency, when operated at a substrate temperature of 200°C. Detailed analysis of the structural, morphological, and optical characteristics of the developed layer revealed a nanoscale dendritic structure and an optical band gap of 2.58 eV. The optimal device showed significant performance advantages at relatively low bias voltages across various wavelengths and illumination powers. Specifically, the device achieved a responsivity (R) of 16.881 μA/W, a specific detectivity (D^*) of $9.25 \cdot 10^{16}$ Jones, and an external quantum efficiency (EQE) of 39.495 at a wavelength of 530 nm, and an illumination power of 50 mW/cm^2. The switching behaviour was characterized by response and recovery times of 0.32 and 0.65 seconds, respectively.

REFERENCES

1. M. S. Hamed and G. T. Mola, *Journal of Alloys and Compounds*, **802**: 252 (2019); https://doi.org/10.1016/j.jallcom.2019.06.108
2. M. Z. Ansari, S. A. Ansari, N. Parveen, M. H. Cho, and T. Song, *New Journal of Chemistry*, **42**, No. 8: 5859 (2018); https://doi.org/10.1039/C8NJ00018B
3. C. Tablero, *The Journal of Physical Chemistry C*, **118**, No. 28: 15122 (2014); https://doi.org/10.1021/jp502045
4. J. Santamaria, E. Iborra, I. Mártil, G. Gonzalez-Diaz, and F. Sanchez-Quesada, *Vacuum*, **37**, Nos. 5–6: 433 (1987); https://doi.org/10.1016/0042-207X(87)90328-9
5. S. de Reguardati, J. Pahapill, A. Mikhailov, Y. Stepanenko, and A. Rebane, *Optics Express*, **24**, No. 8: 9053 (2016); https://doi.org/10.1364/OE.24.009053
6. F. A. Sabah, N. M. Ahmed, Z. Hassan, and H. S. Rasheed, *Procedia Chemis-*

try, **19**: 15 (2016); https://doi.org/10.1016/j.proche.2016.03.005
7. C. Naşcu, I. Pop, V. Ionescu, E. Indrea, and I. Bratu, *Materials Letters*, **32**, Nos. 2–3: 73 (1997); https://doi.org/10.1016/S0167-577X(97)00015-3
8. S. Bashir, N. Iqbal, A. Jamil, A. Alazmi, and M. Shahid, *Ceramics International*, **48**, No. 3: 3172 (2022); https://doi.org/10.1016/j.ceramint.2021.10.090
9. Z. Sun, C. Yi, Z. Hameiri, and S. P. Bremner, *Appl. Surf. Sci.*, **555**: 149727 (2021); https://doi.org/10.1016/j. apsusc.2021.149727
10. H. Wu, J. Yu, G. Yao, Z. Li, W. Zou, X. Li, and Z. Tang, *Sensors and Actuators B: Chemical*, **369**: 132195 (2022); https://doi.org/10.1016/j.snb.2015.01.070
11. M. Xin, K. Li, and H. Wang, *Applied Surface Science*, **256**, No. 5: 1436 (2009); https://doi.org/10.1016/j.apsusc.2009.08.104
12. R. H. Al-Saqa and I. K. Jassim, *Journal of Nanomaterials & Biostructures*, **18**, No. 1: 165 (2022); doi:10.15251/DJNB.2023.181.165
13. Z. Q. Li, J. H. Shi, Q. Q. Liu, Z. A. Wang, Z. Sun, and S. M. Huang, *Applied Surface Science*, **257**, No. 1: 122 (2010); https://doi.org/10.1016/j.apsusc.2010.06.047
14. N. P. Huse, A. S. Dive, K. P. Guttu, and R. Sharma, *Mater. Sci. Semicond. Proc.*, **67**: 62 (2017); https://doi.org/10.1016/j.mssp.2017.05.010
15. J. Han, C. Dong, and S. Shi, *J. Mater. Chem. B*, **8**: 935 (2020); https://doi.org/10.1039/c9tb02597a
16. Z. Zhao, M. Liu, K. Yang, C. Xu, Y. Guan, X. Ma, and F. Zhang, *Advanced Functional Materials*, **31**, No. 43: 2106009 (2021); https://doi.org/10.1002/adfm.202106009
17. X. Li, K. Zhou, J. Zhou, J. Shen, and M. Ye, *J. Mater. Sci. Technol.*, **34**, 2342 (2018); https://doi.org/10.1016/j. jmst.2018.06.013
18. J. Huang and K. Pu, *Chem. Int. Ed. Engl.*, **59**: 11717 (2020); https://doi.org/10.1002/anie.202001783
19. N. Liu, L. Xu, S. Zhou, L. Zhang, and J. Li, *ACS Sens.*, **5**: 3607 (2020); https://doi.org/10.1021/acssensors.0c01910